RESEARCH ARTICLE

An outline of functional self-organization in V1: synchrony, STLR and Hebb rules

J. J. Wright · P. D. Bourke

Abstract A model of self-organization of synapses in the striate cortex is described, and its functional implications discussed. Principal assumptions are: (a) covariance of cell firing declines with distance in cortex, (b) covariance of stimulus characteristics declines with distance in the visual field, and (c) metabolic rates are approximately uniform in all small axonal segments. Under these constraints, Hebbian learning implies a maximally stable synaptic configuration corresponding to anatomically and physiologically realistic ''local maps'', each of macro-columnar size, and each organized as Möbius projections of a "global map" of retinotopic form. Convergence to the maximally stable configuration is facilitated by the spatio-temporal learning rule. A tiling of V1, constructed of approximately mirror-image reflections of each local map by its neighbors, is formed. The model supplements standard concepts of feed-forward visual processing by introducing a new basis for contextual modulation and neural network identifications of visual signals, as perturbation of the synaptic configuration by rapid stimulus transients. On a long time-scale, synaptic development could overwrite the Möbius configuration, while LTP and LTD could mediate synaptic gain on intermediate time-scales.

J. J. Wright (✉)
Department of Psychological Medicine, University of Auckland, Auckland, New Zealand
e-mail: jj.w@xtra.co.nz

J. J. Wright · P. D. Bourke
Brain Dynamics Centre, University of Sydney, Sydney, Australia

P. D. Bourke
Western Australia Supercomputing Project, University of Western Australia, Perth, Australia

Introduction

The striate cortex (V1), which receives direct visual projections from the eyes, is perhaps the most studied area in the neocortex. Analysis of its mechanisms of operation has been a major interest since the work of Hubel and Wiesel (1968, 1977).

Classically, stimulation of a small locale in the visual field [the receptive field (RF)] brings forth neuronal firing about 40–60 ms later, somewhere within a cortical macrocolumn—itself a small part of the striate cortex—corresponding to the position of the RF within the homologous projection of the visual field onto V1 (Hubel and Wiesel 1968). Spatial filtering of signals ascending the visual pathway, consequent to the convergence and divergence of neural signals, and fringe inhibition along the visual pathway is invoked to account for some selective properties of cellular responses in the cortex. The classical viewpoint gives little weight to the role played by lateral connections in V1, which are much more numerous than those of the direct visual pathway. A large body of evidence indicates that these connections add "contextual modulation", modifying the purely feed-forward processes, and affecting the response within each RF (Li et al. 2000; Angelucci et al. 2002; Levitt and Lund 2002; Angelucci and Bullier 2003; Alexander and Wright 2005). The mechanisms of contextual modulation are a subject of ongoing research (Ringach et al. 1997; Chavane et al. 2000; Ernst et al. 2001; Series et al. 2002; Cavanaugh et al. 2002). Recently, Basole et al. (2003) showed that a classic conceptual pillar—the property of Orientation Preference (OP);

the selective response of V1 cells to visual stimuli of particular orientation—was not an invariant and unique property, but is a function of the velocity, relative orientation to direction of movement, and length, of line stimuli.

Contextual modulation as a theoretical problem overlaps with other theoretical problems. These include the role of synchronous oscillation, its putative role in solving "the binding problem" (von der Marlsburg 1973; Eckhorn et al. 1988; Gray et al. 1992a, b; Singer and Gray 1995), determination of the possible categories of local neural network dynamics in visual cortex (Freeman 1975, 2007; Bressloff 2002), the physiology of information storage by synaptic modifications (Artola et al. 1990), and specification of optimum learning rules (Kay and Phillips 1997; Phillips and Singer 1997).

A possible way in which contextual information might be relayed widely in V1 was suggested by Alexander et al. (2004) who proposed the idea that V1 is tiled by many "local maps", each one of which is a compressed representation of a "global map"—the whole, or part of, V1 itself—and therefore a representation of the visual field wider than the RF. This notion was further developed in a theoretical account of the self-organization of synapses during development of V1 (Wright et al. 2006) which deduced the most stable configuration of synapses to emerge under a Hebbian learning rule, and depended upon theoretical analyses of synchronous oscillation (Wright 1997; Robinson et al. 1998; Wright et al. 2000; Chapman et al. 2002) as an organizing principle. That explanation of self-organization of the synaptic connections was deficient in two respects. First, no particular physiological synaptic mechanism was taken as the basis of the Hebbian learning. Second, approach of all synapses to their maximally stable condition was assumed, without any mechanism being proposed to assist convergence towards maximum stability. In the present paper, these deficiencies are partly remedied by appeal to properties of the spatiotemporal learning rule (STLR; Tsukada et al. 1996, 2007; Tsukada and Pan 2005)—which was developed in relation to experimental work on Long Term Potentiation (LTP) and Long Term Depression (LTD) in the hippocampus. We will argue that the modified model may account for the self-organization of lateral connections in V1. We will also indicate ways in which contextual information from surrounding macrocolumns may be input to each macrocolumn—thus complementing the classical, direct, RF pathways.

Initial conditions

The initial conditions are those prevailing at the beginning of visual development, in the perinatal period.

Synaptic densities in V1

In V1 and cortex generally, the density of synaptic couplings generated by each neuron declines with distance from the soma of the cell of origin, at two principal scales—that of the local intra-cortical connections (at the V1 macrocolumnar scale), versus the longer intracortical connections (Scholl 1956; Braitenberg 1978; Braitenberg and Schuz 1991; Liley and Wright 1994). Thus, any macrocolumnar-sized area is both richly locally interconnected, and receives input from a much wider extent of V1.

Visual cross-correlation and synchronous fields

Because of the decline of synaptic density with distance, theory indicates that spatial covariance of activity generated by fields of synchronous oscillation between small groups of pyramidal neurons in V1 must also decline with distance (Wright 1997; Robinson et al. 1998; Chapman et al. 2002). Visual stimuli also exhibit a decline in spatial covariance with distance, and impose this property upon activity in V1, so activity in V1 may be treated as "brown" noise, at both the global, V1, scale, and the local, macrocolumnar, scale. As will be shown, this provides a metric for organization of specific synaptic connections.

Figure 1 shows the initial conditions schematically. Long-range polysynaptic connections carry signals from all, or a large part of V1, dispersing their synapses throughout each and every area of macro-columnar size, generating transient fields of synchrony.

Learning rules

The spatiotemporal learning rule (STLR)

The spatiotemporal rule has been recently specified in relation to LTD/LTP (Tsukada et al. 2007). It specifies the way that afferent synapses to a post-synaptic neuron cooperate to mutually strengthen synaptic weights. Following the terminology of Tsukada et al. (2007), ΔW_{ij}, the change in weight of a synapse from a pre-synaptic neuron i to a postsynaptic neuron j is given by

$$\Delta W_{ij} = \eta \cdot h \left(\sum_{m=0}^{n} I_{ij}(t_m) e^{-\lambda_2(t-t_{n-m})} - \theta \right) \quad (1)$$

where η is a learning rate coefficient, $h(u)$ is a sigmoid function of the Potentiation force, for which θ is the threshold and $\lambda_2 \approx 223$ ms is the time decay constant of temporal summation.
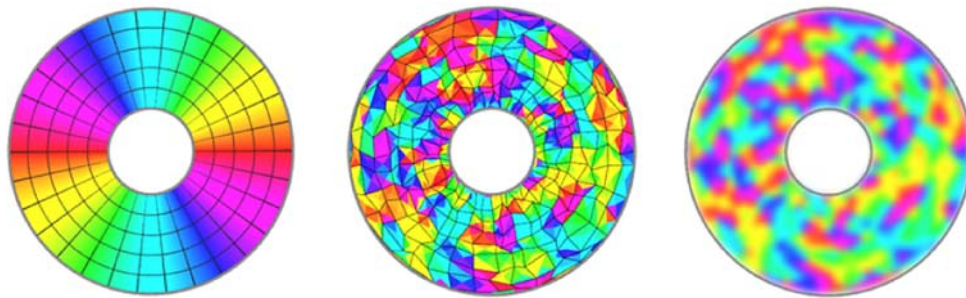
Fig. 1 Initial conditions for local evolution of synaptic strength. *Left* The global field (V1) in polar co-ordinates. Central defect indicates the position of a local area of macro-columnar size. Polar angle is shown by the color spectrum, twice repeated. *Middle* Zones of random termination (shown by color) of lateral axonal projections from global V1 to any single local area of macro-columnar size. (The central defect is an arbitrary zero reference.) *Right* Transient patterns of synchronous oscillation generated in the local area, mediated by local axonal connections

$$\exp\left[-\lambda_2(t - t_{n-m})\right] \tag{2}$$

is the time-history of the change in synaptic weights, and

$$I_{ij}(t) = w_{ij}(t)x_i(t)\sum_{k \neq i}(w_{kj}(t)x_k(t)) \tag{3}$$

is the cooperative activity. In Eq. 3, $w_{ij}(t)$ is the value of a weight from neuron i to neuron j prior to adjustment, $x_i(t)$ is the excitatory activity of the ith afferent neuron, and $\sum_{k \neq i}(w_{kj}(t)x_k(t))$ is the weighted corollary activity in other neurons afferent to j.

Conventional Hebbian LTP/D

In association with STLR, Tsukada et al. (2007) have described a concurrent Hebbian form of synaptic modification, which they abbreviate as HEBB. Their findings can be approximated using a simple Hebb rule applied in Wright et al. (2006). Where $r_{Q\varphi}$ is the "effective" coincidence of the pre- and post-synaptic neurons

$$r_{Q\varphi} = \frac{Q_{\max}}{n}\sum_t Q_e(t) \times \varphi_e(t + \Delta) \\ Q_e(t) \in \{0, 1\}; \varphi_e(t) \in \{0, 1\} \tag{4}$$

$Q_{\max}$ is the maximum action potential firing rate of pyramidal neurons;
$Q_e(t)$ is the firing state of the post-synaptic neuron, and
$\varphi_e(t)$ is the firing state of the pre-synaptic neuron.

$\Delta = n\tau$, where τ is a time-step, is a time window, some tens of ms in duration in which increase of Hebbian synaptic gain can occur if $Q_e = \varphi_e = 1$ during this window. If Δ is negative—that is, pre-synaptic spike precedes post-synaptic spike—then LTP ensures. If Δ is positive, LTD ensues. For simplicity, here we assume no active process is involved in LTD, but merely an absence of Hebbian consolidation.

The steady-state HEBB gain factor is

$$H_s = H_{\max}\exp[-\lambda/r_{Q\varphi}] \quad \lambda + ve \tag{5}$$

where λ is a suitable constant. The rise and fall of synaptic gain in response to a brief period of high pre-post synaptic coincidence within the appropriate time window is described by the normalized impulse response function

$$H(t) = H_s(t - \tau) \otimes \frac{(\beta - \alpha)}{\alpha\beta}(\exp[-\beta\tau] - \exp[-\alpha\tau]) \tag{6}$$

where α and β are rise and fall time constants. As well as LTP/D, this simple time–response could include further mechanisms of synaptic consolidation by introducing a set of λ, α, β applicable at different time-scales.

Synaptic evolution

The STLR and HEBB rules are complementary. We will first show that the HEBB rule is sufficient to define stable end-points of synaptic modification, and then show that STLR assists convergence to the stable end-points.

Hebbian stability at individual synapses

Since pre- and post-synaptic firing rates approximate Poisson processes, the variance, $\varsigma^2(r_{Q\varphi}, \tau)$, of pre-post synaptic coincidence measured during short epochs, τ, is proportional to the mean value, over a set of epochs, i.e.,

$$\zeta^2(r_{Q\varphi}, \tau) \propto \bar{r}_{Q\varphi} \tag{7}$$

From this it can be shown (Wright et al. 2006) that $S(\bar{r}_{Q\varphi}, t)$, the RMS variation of HEBB synaptic gain around the steady-state value (Eq. 5), has a single maximum at $\bar{r}_{Q\varphi} = 2\lambda/3$, and zero minima at $\bar{r}_{Q\varphi} = 0, \infty$. Therefore, stable states of the synapse can occur only at either maximum saturation or zero saturation. We will subsequently refer to maximally saturated synapses as *saturated* and zero-saturated synapses as *sensitive*. Following Tsukada et al. (2007) we can

provisionally associate the saturated state with LTP and the sensitive state with LTD, for the appropriate time-scale.
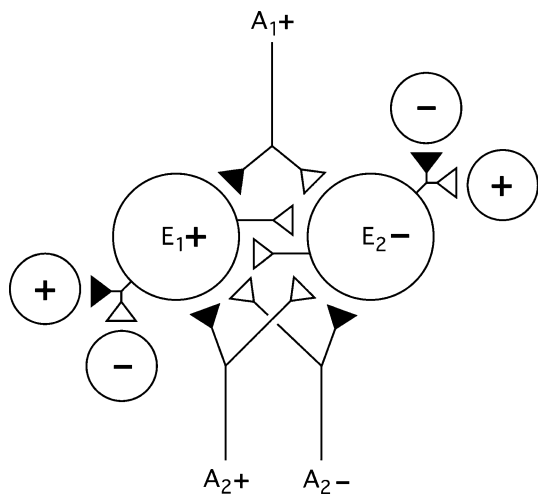
Metabolic uniformity

Competition occurring for metabolic resources within axons adds a constraint (Grossberg and Williamson 2001). Metabolic energy supply of all small axonal segments remains approximately uniform, while the metabolic demand of saturated synapses, which have high activity, will be much greater than for sensitive synapses. Therefore, the proportion of saturated and sensitive synapses must be approximately uniform along axons.

Figure 2 shows schematically how metabolic uniformity restricts the way saturated and sensitive connections can form between neurons of high and low average firing covariance. In concert with both the Hebbian and STRL learning rules, the metabolic constraint imposes a particular form upon the stable synaptic configuration throughout V1, as will next be described.

The impact of distance/density and saturation/ sensitivity on Hebbian synaptic stability

All positions in V1, $\{P_{j,k}\}$, can be given an ordered numbering in the complex plane, $1...j,...k,...,2n$, and all positions within a macrocolumn located at P_0, $\{p_{j,k}\}$, can be

Fig. 2 Architectural constraints implicit in metabolic uniformity, at synaptic stability. E1 and E2 are closely situated neurons in a macrocolumn. A1 and A2 are afferent axons from elsewhere in visual cortex. Black triangles indicate saturated synapses, white triangles sensitive synapses. Metabolic uniformity requires A1+, A2+ and A2− to establish both sensitive and saturated synapses in any small volume. Compatible stable solutions for positively correlated inputs from A1+ and A2+, and also from the negatively correlated A2−, are shown. Consequently E1 and E2 must have negatively correlated activity, and, in turn, must link to each other via sensitive synapses, and map via sensitive and saturated synapses to further adjacent neurons

similarly numbered. The total perturbation of synaptic gains for the synapses arising from V1 and entering the macrocolumn, $\Psi(pP)$, and the total perturbation of synaptic gains within the macrocolumn, $\Psi(pp)$, can thus be written as

$$\Psi(pP) = \sum_{j=1}^{j=n} \sum_{k=1}^{k=n} \sigma_{SAT}(p_jP_k)S_{SAT}(p_jP_k)$$
$$+ \sum_{j=1}^{j=n} \sum_{k=1}^{k=n} \sigma_{SENS}(p_jP_k)S_{SENS}(p_jP_k) \qquad (8)$$

$$\Psi(pp) = \sum_{j=1}^{j=n} \sum_{k=1}^{k=n} \sigma_{SAT}(p_jp_k)S_{SAT}(p_jp_k)$$
$$+ \sum_{j=1}^{j=n} \sum_{k=1}^{k=n} \sigma_{SENS}(p_jp_k)S_{SENS}(p_jp_k) \qquad (9)$$

where $\sigma_{SAT}(p_jP_k, p_jp_k)$ and $\sigma_{SENS}(p_jP_k, p_jp_k)$ are densities of synapses, respectively, approaching the saturated and sensitive states, and $S_{SAT}(p_jP_k, p_jp_k)$ and $S_{SENS}(p_jP_k, p_jp_k)$ are the corresponding variations of synaptic gains over a convenient short epoch.

Since densities of synapses decline with distances of cell separation, then as a simple arithmetic property of sums of products, minimization of $\Psi(pp)$ requires synapses connecting neurons separated by short distances to most closely approach either maximum saturation or maximum sensitivity, while remaining in a constant ratio, according to metabolic uniformity. Sensitive synapses must link pre- and post-synaptic neurons with minimal pre- and post-synaptic pulse coincidence, and the reverse is true for saturated synapses. Therefore, the saturated and sensitive synapses originating from any pre-synaptic neuron must respectively link to different, yet closely adjacent, post-synaptic neurons. Similarly, minimization of $\Psi(pP)$ requires that saturated connections afferent to any p_j arise from highly covariant, and therefore closely situated, sites in V1, while sensitive connections afferent to p_j must arise from well separated sites, yet metabolic uniformity requires that equal ratios of sensitive and saturated pre-synapses arise from cells at any single site. Again, the saturated and sensitive synapses arising from any pre-synaptic neuron must respectively link to different, while closely adjacent, sets of cells with low firing covariance between to the two groups of post-synaptic cells, as indicated in Fig. 2. These constraints can be met as follows.

Möbius projection, and the local map

By re-numbering $\{P_{j,k}\}$ as $\{P_{j1,j2,k1,k2}\}$, and $\{p_{j,k}\}$ as $\{p_{j1,j2,k1,k2}\}$ the subscripts $1,...j1,...j2,...,n,(n + 1),...,j2, ...,k2,...,2n$ can be ascribed in the global map so that $j1$ and $j2$ are located diametrically opposite and equidistant from P_0, while in the local map $j1$ and $j2$ have positions analogous to superimposed points located on opposite surfaces

of a Möbius strip. This enables definition of a *Möbius projection* (the *input map*) from global to local, and a *Möbius ordering* within the local map. That is,

$$\frac{P_{jm}^2}{|P_{jm}|} \rightarrow p_{km} \quad m \in \{1, 2\} \tag{10}$$

$$p_{jm} \rightarrow p_{km} \quad m \in \{1, 2\} \tag{11}$$

In Eq. 10, the mapping of widely separated points in the global map converge to coincident points on opposite surfaces of the local map's Möbius representation. In the Eq. 11 the density of saturated synaptic connections now decreases as $|j1 - k1|$ and $|j2 - k2|$, while the density of sensitive couplings decreases as $|j2 - k1|$ and $|j1 - k2|$. This meets mathematically the constraints of minimization of Eqs. 8 and 9. The anatomical realization requires $j1$ and $j2$ in the local map to represent two distinct groups of neurons. To attain maximum synaptic stability within the local map an intertwined mesh of saturated couplings forms, closed after passing twice around the local map's center, with sensitive synapses locally linking the two turns of the mesh together. In this fashion both saturated and sensitive synapses decline in density with distance, as required. The input map is of corresponding form, conveying an image of the activity in V1 analogous to projection onto a Möbius strip.

The stable configuration for saturated synapses is shown in Fig. 3.

An identical map, but with complementary colors to those of the input and local maps of Fig. 3 could be drawn for sensitive synapses.

Monosynaptic interactions between adjacent local maps

The input and local maps can, in principle, emerge with any orientation, and with either left- or right-handed chirality. However, chirality and orientation of adjacent local maps is also constrained by requirement for overall stability. Adjacent local maps should form in approximately mirror image relation, as shown in Fig. 4, because in that configuration homologous points within the local maps have densest saturated and sensitive synaptic connections, thus meeting minimization requirements analogous to those of Eqs. 8 and 9.

Role of STLR

Independent of considerations arising from the Hebb rule, the STLR rule, applied in metabolic uniform conditions, also leads similar synaptic maps to those of Eqs. 10 and 11 and Fig. 3. Under STLR, synaptic stability is reached to satisfy the following requirements.

* All neurons in the global map must give rise to some saturated synapses, so the input map must be *complete* in the sense that the whole global map is represented in the input map.
* Since the spatio-temporal rule requires the mutual strengthening of synapses afferent to a small locale to increment preferentially when they arise from maximally covariant inputs, and since covariance declines with distance in the global map, the input map must be a *spatially continuous* representation of the global map.
* To be both spatially continuous and complete, the input map must be topologically identical to the mapping

$$\frac{P_j^N}{|P_j|} \Rightarrow p_j \tag{12}$$

(Note that there are no implied constraints on either the reference zero, the angular orientation of the axes, or the chirality of plane $\{p\}$ in this mapping.)
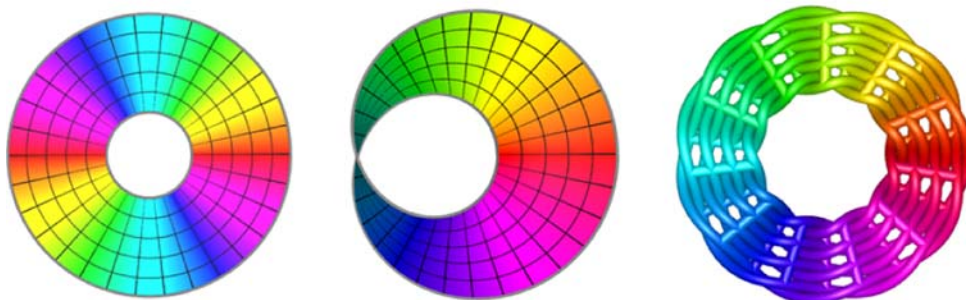
Fig. 3 Evolution of synaptic strengths to their maximally stable configuration. *Left* The global field (V1), as represented in Fig. 1. *Middle* Saturated synaptic connections input from the global field now form a Möbius projection of the global field, afferent to the local map, forming an input map. *Right* Saturated local synapses within the local map form a mesh of connections closed over $0 - 4\pi$ radians.

The central defect now corresponds to the position within the local map, of the local map within the global map. Sensitive synapses (not shown) link adjacent neurons as bridges between the $0 - 2\pi$ and $2\pi - 4\pi$ limbs of the mesh of saturated connections. (From Wright et al. 2006)
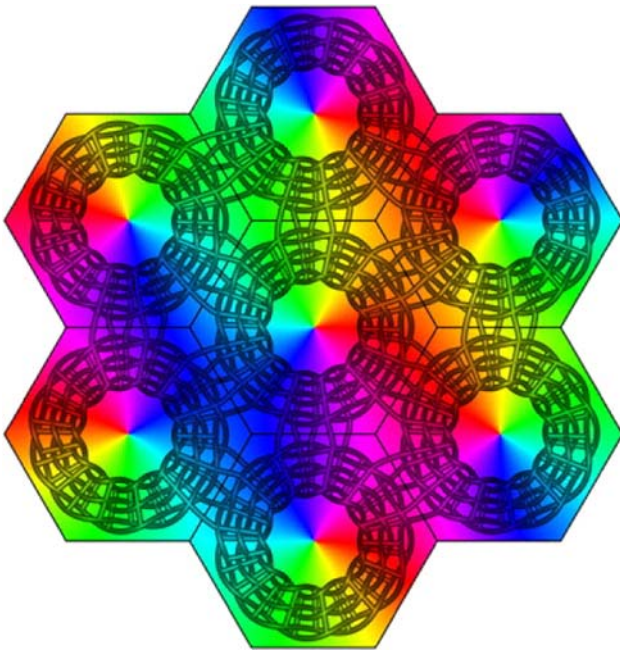
Fig. 4 Organization of saturated coupling within and between local maps, and the approximate mirror symmetry of orientation preference in adjacent local maps. (Wright et al. 2006)

- As indicated in Fig. 2, the metabolic constraint requires that many closely situated pairs of neurons in $\{P\}$ must have low covariances, and therefore must receive afferent signals of low covariance. This can occur only if the pre-synapses reaching them from $\{P\}$ arise from neuron cell bodies as far apart as possible. Therefore, in Eq. 12 $N = 2$, in which case as widely separated points in $\{P\}$ as possible are mapped to identical points on opposite side of a Möbius strip representation of $\{p\}$. The "opposite sides of a Möbius strip" can be considered to be neurons in the macrocolumn which, although closely adjacent, have only sensitive synaptic couplings.
- By similar arguments, connections within and between macrocolumns would form under STLR in the same configurations as are implied by the Hebb rule.

Thus, the Hebb and STLR rules appear to be complementary, each implying convergence toward the same most stable state.

Comparisons to experiments

No demonstration of V1 connectivity of Möbius configuration is known. Direct proof would require demonstration of connections closed over 4π. This is a technically difficult proposition, complicated by a remaining theoretical problem—namely, the uncertainty of the most appropriate

time-scale over which to describe the synapses as "saturated" or "sensitive". Time scales faster than LTP/D, to those as slow as synaptic pruning, may be appropriate. It is also possible that the Möbius configuration may be a transient developmental condition, subsequently overwritten by dynamical changes related to mature visual processing. For the present, indirect evidence, some of which is described below, indicates consistency of the hypothetical model with experimental data.

Evolution of visual maps

For present purposes OP may be equated with the stimulation by a line in the visual field, of a correspondingly oriented group of interconnected neurons in the local map. (Specific individual neuronal response preferences for a line of a specific orientation, under various combinations of line angle of attack, velocity, and length, can be shown to be a property of the wave theories on which this model is based. This effect will be reported in detail elsewhere.)

OP emerges in early development of the brain, around the neonatal period (Blakemore 1976; Chapman et al. 1996). Figures 5a–c, show stages in the simulated evolution of OP in V1.

As the initial condition (Fig. 5a) pairs of adjacent mirror-image color-wheels were placed in random positions in the frame, as indicated by the solid black lines. These initial pairs represent local maps that have developed early. These pairs then seed subsequent organization amongst later evolving local maps (see Wright et al. 2006). The emerging form of OP in Fig. 5 is plausibly comparable to experimental data, as described in newborn ferrets (Chapman et al. 1996).

This procedure reproduces typical topographies of orientation preference maps, as can be seen by comparison of simulated (Fig. 6a) and real data (Fig. 6b). Linear zones, saddle points and occasional additional aberrant singularities (which do not correspond to centers of local maps) appear as junctions where differently seeded zones intersect, while preservation of some of the idealized orderly mirroring diagrammed in Fig. 5 is seen in both real and simulated data.

As discussed earlier, mutual organization among local maps as diagrammed in Fig. 4 results in saturated synaptic connections between homologous points. In accord with this expectation, linkage between cells of similar orientation preference should occur between local maps, and does so in fact (Bosking et al. 1997), as is shown in Fig. 6b.

Ocular dominance columns

In binocular animals OP maps are organized into ocular dominance (OD) columns (Obermayer and Blasdel 1993;
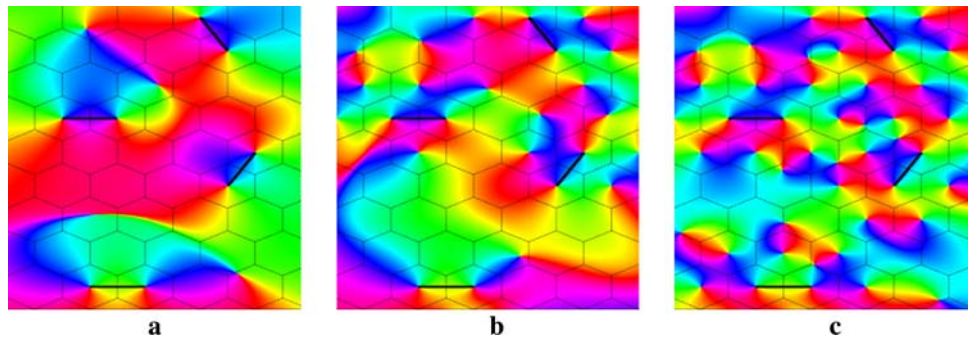
Fig. 5 (**a**) Early development of OP. Black bars indicate early pairs of local maps with mirror-image symmetry. Between these maps the initial OP of cells is biased by the influence of the early maps. (**b**) Later, more completed local maps have formed up adjacent to the early maps. The expanded set of complete local maps continues to bias the orientation and chirality of emerging maps. (**c**) Continuation toward the completed state shown in Fig. 6a

Fig. 6 Simulated and real maps of orientation preference. (**a**) Final configuration of OP consequent to seeding the development of fields of OP with the local map mirror-image pairs shown joined by solid lines. (**b**) Real OP as visualized in the tree shrew by Bosking et al. (1997) Intracortical connections superimposed in black connect zones of like OP
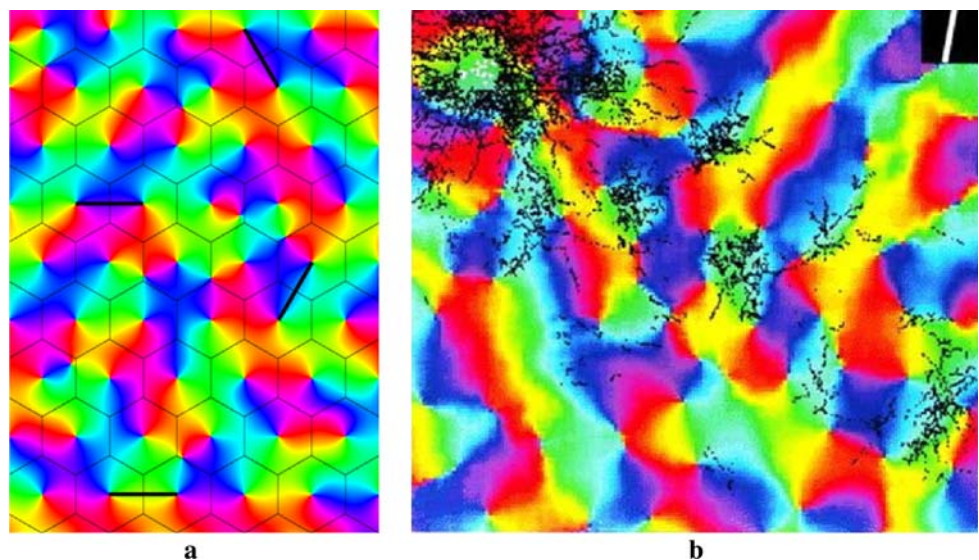
Swindale et al. 2000). Adjacent macrocolumns responsive to either the left or right eye alternate, organized into parallel columns for each eye. Singularities tend to lie at the centers of each OD column, and OP linear zones cross the boundary between OD columns orthogonally to the boundary. OD columns can be explained as a special case of the operation of the same rules of evolution of synaptic connections.

The visual information delivered to V1 from the two eyes arises from overlapping projections of the visual field because of the lateral separation of the eyes. Consequently spatial cross-correlation is not a declining function of distance of separation in the visual field, in the binocular projection to V1. In this altered circumstance maximum stability may be reached by suppressing input from opposite eyes in adjacent local maps, each sharing closely similar inputs, and individually conforming to the inverse distance/covariance relation. Figure 7a, b show comparison of simulated and real OD columns.

Consequences of lagged transmission from the global to the local map

Mention was made in the Introduction of the findings of Basole et al. (2003) who have shown OP to be a function of line stimulus velocity, relative orientation to direction of movement, and length. In the present model these properties arise naturally from a consideration of conduction lags in V1. Signals conveyed laterally within V1, initiated by direct RF inputs to more remote macrocolumns, act to prime a particular macrocolumn by sub-threshold bombardment, while the direct RF input acts to trigger local cell activity above firing threshold. Axonal conduction lags from the global to the local maps can then account for dynamic variation of OP, as indicated in Fig. 8.

If a neuron in some RF has an OP of ψ, as measured in a classical fashion using a slowly moving line oriented at right angles to its direction of passage across the visual field, then it will apparently have an OP of $\psi + \Delta\psi$, where

Fig. 7 (**a**) Results of simulating development of OD columns (Wright et al. 2006). (**b**) Real OD columns, as visualized by Obermayer and Blasdel (1993)
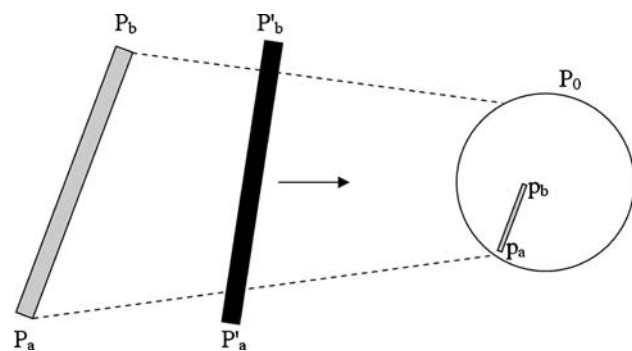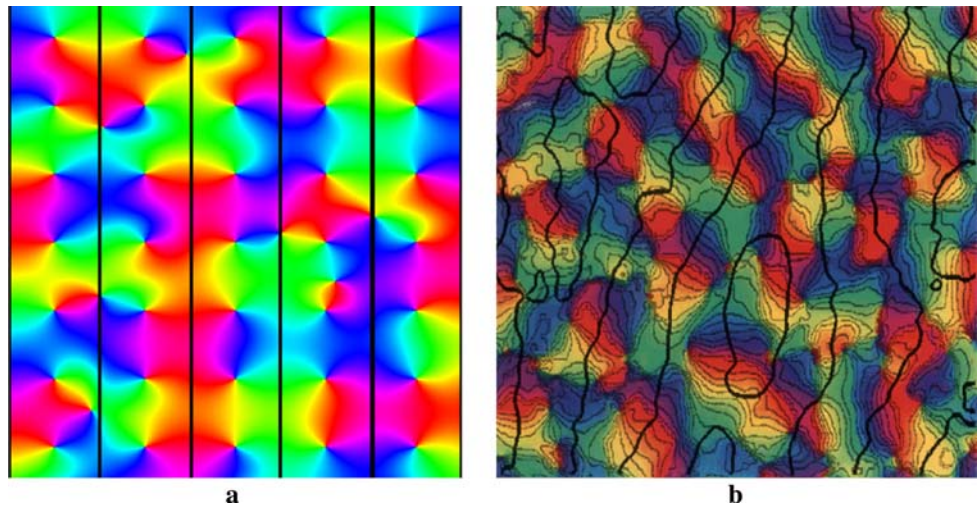
Fig. 8 Conditioning of receptive field OP by moving textures in the global field. Grey semitone bars, $P_a P_b$ and $p_a p_b$ represent corresponding positions in the global and local maps, respectively. The black bar $P'_a P'_b$ is a texture element moving to straddle the local map at P_0, and which has crossed P_a and P_b so as to generate trans-cortical signals which reach P_0 simultaneously

$$\Delta\psi = \sin^{-1}\left[\sin(\pi - \omega)\left|\frac{\mathbf{v}}{\upsilon}\right|\left(|P_a - P_0| - |P_b - P_0|\right)/|P_a - P_b|\right]$$
(13)

The moving line is oriented at an angle ω with respect to the direction of passage, travels with a velocity v, has an approximate length $\left|P'_a - P'_b\right|$, and crosses a line in the global map between P_a and P_b on its way to cross the RF situated at P_0. The velocity of electrocortical wave conduction is υ. Equation 13 conforms qualitatively to the experimental results (Basole et al. 2003; Wright et al. 2006) and offers prospect of quantitative tests.

Implications for cortical information processing

The classical RF and the Möbius local map

A straight-line visual stimulus has a two-fold rotational symmetry, which is why OP is defined on a range $0–\pi$, yet

can be mapped circumferentially around a singularity over $0–2\pi$. The local map also has an angle-doubling property in the folding of the global map onto the local map. Thus, the classical receptive field and the local map can achieve congruence, bringing together direct information and contextual information.

Uniqueness of inputs and contextual processing

The dependence of OP upon object velocity, angle of attack, and length is disconcerting for classic views of the selectivity of visual neurons, since it implies that many stimuli with different characteristics could all optimally stimulate the same neuron. However, problems of signal ambiguity are not apparent in the present model. Figure 9 shows how any point on a stimulus moving in the visual field will generate laterally propagating waves in V1, which will arrive with different conduction delays at homologous points in many local maps. Neurons at the homologous points can form a synchronous field, and inputs to the synchronous field will be unique for the particular size, position, and velocity of the stimulus. Thus, the Möbius mapping can act to convey unambiguous contextual information to the local RF from some substantial extent of V1. Congruence of the feed-forward representation of a stimulus currently within the RF, with contextual signals conveyed to the local map, which were generated by the same stimulus at earlier positions on its locus, would enable the feed-forward inputs to act as confirmatory signals, often critical to initiation of cell firing within a specific macrocolumn.

Fast attractor dynamics

At time-scales faster than modification of synaptic gain by LTP and LTD, the Möbius representation of the global field

Fig. 9 Synchronous fields among homologous points in local maps. *Left* Each point on the cortical image of a moving bar projected to V1 generates signals arriving at homologous points on numerous local maps with different delays, characterizing the cortical image. *Right* Homologous points in neighboring local maps enter into image-specific synchronous oscillation
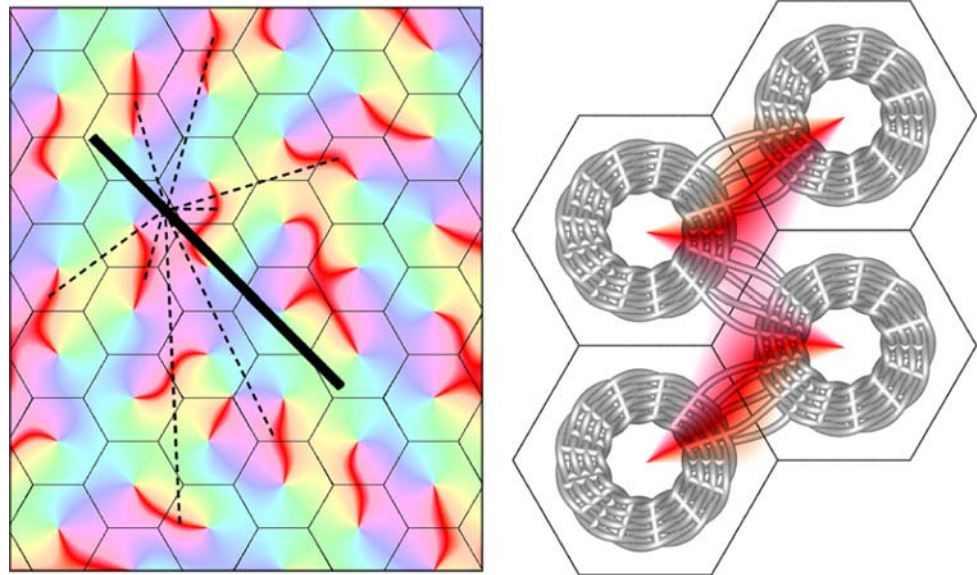
within each local map would be subject to transient perturbations induced by all visual stimuli. A typical perturbation and recovery from this state, such as would be induced by a straight-line moving across the RF is shown in Fig. 10. Since the local network has a single fixed point attractor, perturbation by contextual and RF inputs will lead to unique locii in phase space as the local network responds to specific stimuli.

Evolution of the map under slower learning processes

We have assumed that on a time-scale appropriate for synaptic evolution under STLR and HEBB, stimuli in the visual field can be approximated as brown noise. However, as neural development advances, this assumption is unlikely to be true other than as first approximation, and higher order statistical associations in visual stimuli will therefore result in departures from the pure Möbius configuration. Breakdowns of the basic configuration could thus store

information about higher order statistics of the visual field—for example, predominance of lines of a particular orientation. Slow changes of this type, perhaps related to synaptic growth, correspond to persistence of the perturbation shown in Fig. 10. This secondary process could explain the results of visual deprivation experiments (Blakemore 1976).

Conclusion

The STL and HEBB rules and synchronous oscillation together permit a consistent account of self-organization in the visual cortex, which supplements both classical feed-forward explanations (Hubel and Wiesel 1968) and recent models of local lateral interaction in V1 (Grossberg and Williamson 2001). Unique patterns of input signals bearing contextual information can be generated by any specific object moving in the visual field and conveyed more
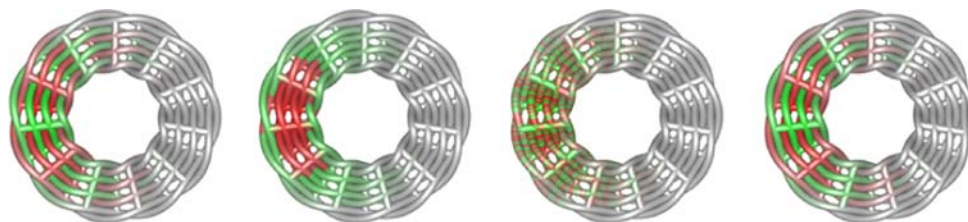
Fig. 10 Effects of perturbation. *Left* A representation of the connections formed by a small group of neurons with cell bodies located at 3o'clock in the local map. Saturated connections (red) and sensitive connections (green) are arrayed at their maximally stable configuration. *Second from left* An afferent volley is delivered to neurons at 3o'clock in the local map, arising from sites on both sides of the

position of the local map, so that neurons in the $0 - 2\pi$ and $2\pi - 4\pi$ limbs of the mesh are forced into highly correlated firing. *Second from right* On withdrawal of the perturbing afferent volley, the synaptic configuration generated by the perturbation begins to decay. *Right* The maximally stable configuration is again attained

widely than by the RF alone. Cooperative interactions among macrocolumns could thus process spatial and temporal visual information of complexity much greater than feature extraction per se. The model's implications for local network dynamics require further exploration, including consideration of onset and offset of synchrony (Wright 2008), of neuronal dynamic coding (Tsuda and Kuroda 2004) and storage of information (Kay and Phillips 1997; Phillips and Singer 1997).

The present model leaves open many areas for testing and further development. We have already indicated uncertainty on the degree to which subsequent learning, with multiple mechanisms at different time-scales, and higher-order statistics of visual signals might lead to overwriting of the Möbius configuration. The model may also be applicable outside V1. For example, the special case of segregation of information flows in OD columns might be further reflected in the segregation of information flows in higher visual areas of the dorsal and ventral visual streams. Consideration has not yet been given to interaction of V1 with higher visual areas. Repetition of the principles of mapping of the visual field to V1 might also hold for the interaction of V1 with higher centers, iterating the process of local tiling of higher cortical area with mini-maps of the whole, and raising considerations for "top–down" versus "bottom–up" control processes in the brain.

References

Alexander DM, Wright JJ (2005) The maximum extent of horizontal integration in monkey V1. Vision Res 23(5):721–728

Alexander DM, Bourke PD, Sheridan P, Konstandatos O, Wright JJ (2004) Intrinsic connections in tree shrew V1 imply a global to local mapping. Vision Res 44:857–876

Angelucci A, Bullier J (2003) Reaching beyond the classical receptive field of V1 neurons; horizontal or feedback axons? J Physiol (Paris) 97:141–154

Angelucci A, Levitt JB, Walton EJS, Hupe J-M, Bullier J, Lund JS (2002) Circuits of local and global signal integration in primary visual cortex. J Neurosci 22:8633–8646

Artola A, Brocher S, Singer W (1990) Different voltage-dependent thresholds for the induction of long-term depression and long-term potentiation in slices of the rat visual cortex. Nature 47:69–72

Basole A, White LE, Fitzpatrick D (2003) Mapping multiple features of the population response of visual cortex. Nature 423:986–990

Blakemore C (1976) Modification of visual function by early visual experience. Bull Schweiz Akad Med Wiss 32:13–28

Bosking WH, Zhang Y, Schofield B, Fitzpatrick D (1997) Orientation selectivity and the arrangement of horizontal connections in tree shrew striate cortex. J Neurosci 17(6):2112–2127

Braitenberg V (1978) Cortical architectonics: general and areal. In: Brazier MAB, Petsch H (eds) Architectonics of the cerebral cortex. Raven Press, New York, pp 443–465

Braitenberg V, Schuz A (1991) Anatomy of the cortex: statistics and geometry. Springer-Verlag, New York

Bressloff PC (2002) Bloch waves, periodic feature maps and cortical pattern formation. Phys Rev Lett 89:088101

Cavanaugh JR, Bair W, Movshon JA (2002) Nature and interaction of signals from the receptive field center and surround in Macaque V1 neurons. J Neurophysiol 88(5):2530–2546

Chapman B, Stryker MP, Bonhoeffer T (1996) Development of orientation preference maps in ferret primary visual cortex. J Neurosci 16:6443–6453

Chapman CL, Bourke PD, Wright JJ (2002) Spatial eigenmodes and synchronous oscillation: coincidence detection in simulated cerebral cortex. J Math Biol 45:57–78

Chavane F, Monier C, Bringuier V, Baudot P, Borg-Graham L, Lorenceau J, Fregnac Y (2000) The visual cortical association field: a gestalt concept or a psychophysiological entity? J Physiol (Paris) 94:333–342

Eckhorn R, Bauer R. Jordon W, Brosch M, Kruse W, Monk M, Reitboeck HJ (1988) Coherent oscillations: a mechanism of feature linking in the in the visual cortex? Biol Cybern 60:121–130

Ernst UA, Pawelzik KR, Sahar-Pikielny C, Tsodyks MV (2001) Intracortical origin of visual maps. Nat Neurosci 4(4):431–436

Freeman WJ (1975) Mass action in the nervous system. Academic Press, New York

Freeman WJ (2007) Proposed cortical shutter in cinematographic perception. In: Kozma R, Perlovsky L (eds) Neurodynamics of cognition and consciousness. Springer, New York

Gray CM, Engel AK, Konig P, Singer W (1992a) Synchronization of oscillatory neuronal responses in cat striate cortex: temporal properties. Vis Neurosci 8:337–347

Gray CM, Konig P, Engel AK, Singer W (1992b) Oscillatory responses in cat visual cortex exhibit intercolumnar synchronization which reflects global stimulus properties. Nature 388:334–337

Grossberg S, Williamson JR (2001) A neural model of how horizontal and interlaminar connections of visual cortex develop into adult circuits that carry out perceptual grouping and learning. Cereb Cortex 11:37–58

Hubel DH, Wiesel TN (1968) Receptive fields and functional architecture of the monkey striate cortex. J Physiol 195:215–243

Hubel DH, Wiesel TN (1977) Functional architecture of macaque monkey visual cortex. Proc R Soc (B) 198:1–59

Kay J, Phillips WA (1997) Activation functions, computational goals and learning rules for local processors with contextual guidance. Neural Comput 9:763–778

Levitt JB, Lund JS (2002) The spatial extent over which neurons in macaque striate cortex pool visual signals. Vis Neurosci 19:439–452

Li W, Their P, Wehrhahn C (2000) Contextual influence on orientation discrimination of humans and responses of neurons in V1 of alert monkeys. J Neurophysiol 83:941–954

Liley DTJ, Wright JJ (1994) Intracortical connectivity of pyramidal and stellate cells: estimates of synaptic densities and coupling symmetry. Network 5:175–189

Obermayer K, Blasdel GG (1993) Geometry of orientation and ocular dominance columns in monkey striate cortex. J Neurosci 13(10):4114–4129

Phillips WA, Singer W (1997) In search of common foundations for cortical computation. Behav Brain Sci 20:657–722

Ringach DL, Hawken MJ, Shapley R (1997) Dynamics of orientation tuning in macaque primary visual cortex. Nature 387:281–284

Robinson PA, Rennie CJ, Wright JJ (1998) Synchronous oscillations in the cerebral cortex. Phys Rev E 57:4578–4588

Scholl DA (1956) The organization of the cerebral cortex. Wiley, New York

Series P, Georges S, Lorenceau J, Fregnac Y (2002) Orientation dependent modulation of apparent speed: a model based on the dynamics of feed-forward and horizontal connectivity in V1 cortex. Vision Res 42:2781–2797

Singer W, Gray CM (1995) Visual feature integration and the temporal correlation hypothesis. Ann Rev Neurosci 18:555–586

Swindale NV, Shoham D, Grinvald A, Bonhoeffer T, Hubener M (2000) Visual cortical maps are optimised for uniform coverage. Nat Neurosci 3(8):822–826

Tsuda I, Kuroda S (2004) A complex systems approach to an interpretation of dynamic brain activity II: does Cantor coding provide a dynamic model for the formation of episodic memory? In: Erdi P et al (eds) Cortical dynamics, LNCS 3146. Springer-Verlag, Berlin, Heidelberg, pp 129–139

Tsukada M, Pan X (2005) The spatio-temporal learning rule and its efficiency in separating spatiotemporal patterns. Biol Cybern 92:139–146

Tsukada M, Aihara T, Saito H (1996) Hippocampal LTP depends on spatial and temporal correlation of inputs. Neural Netw 9:1357–1365

Tsukada M, Yamazaki Y, Kojima H (2007) Interaction between the spatiotemporal learning rule (STRL) and Hebb type (HEBB) in single pyramidal cells in the hippocampal CA1 area. Cogn Neurodyn 1:1871–4080

von der Marlsburg C (1973) Self-organization of orientation selective cells in the striate cortex. Kybernetic 14:85–100

Wright JJ (1997) EEG simulation: variation of spectral envelope, pulse synchrony and 40 Hz oscillation. Biol Cybern 76:181–184

Wright JJ (2008) Generation and control of cortical gamma: findings from simulation at two scales. Neural Networks (in press)

Wright JJ, Bourke PD, Chapman CL (2000) Synchronous oscillation in the cerebral cortex and object coherence: simulation of basic electrophysiological findings. Biol Cybern 83:341–353

Wright JJ, Alexander DM, Bourke PD (2006) Contribution of lateral interactions in V1 to organization of response properties. Vision Res 46:2703–2720